A Fault Detection and Isolation Scheme for Lateral Vehicle Dynamics of EVs using a Quantitative Parity Space Approach

Alexander Viehweider
Dept. of Advanced Energy
Grad. School of Frontier Sc.
Hori Fujimoto Laboratory
The University of Tokyo
Kashiwa, Japan 277-8561
viehweider@ieee.org

Kanghyun Nam
Dept. of Electr. Engineering
Hori Fujimoto Laboratory
The University of Tokyo
Tokyo 113-8656, Japan
nam@hori.k.u-tokyo.ac.jp

Hiroshi Fujimoto
Dept. of Advanced Energy
Grad. School of Frontier Sc.
Hori Fujimoto Laboratory
The University of Tokyo
Kashiwa, Japan 277-8561
fujimoto@k.u-tokyo.ac.jp

Yoichi Hori
Dept. of Advanced Energy
Grad. School of Frontier Sc.
Hori Fujimoto Laboratory
The University of Tokyo
Kashiwa, Japan 277-8561
hori@k.u-tokyo.ac.jp

***Abstract*—Advanced control concepts for electric vehicles assume the correct functioning of sensors. In this contribution the problem of sensor failure detection and isolation in the case of lateral vehicle dynamics of EVs is tackled. The method depends on only basic vehicle parameters and assumes only a single failure in the vehicle system. A single sensor failure can be detected and the false alarm rate is minimized. The approach is based on the parity space method implemented with residual observers. Noise of sensors is taken into account and appropriate bounds in the feature space are derived in order to get a robust fault detection indicator. Simulation results and an experimental setup show the validity of the approach.**

I. Introduction

Electric Vehicles (EVs) with In-Wheel-Motors (IWMs) and advanced sensors like Lateral Tire Force Sensors (LTFS) offer great advantages for the control of the vehicle dynamics. Lateral vehicle dynamics can become very precise and there are new opportunities for a real ”3D” motion control scheme [10]. The high degree of freedom that an electric vehicle with 4 independent driven wheels and Active Front Steering (AFS) and Active Rear Steering (ARS) can be exploited in a very efficient way satisfying different constrains and optimality criteria at the same time [7] [13]. The use of lateral tire force sensors together with different acceleration and angle rate sensors allows to estimate unknown parameters and disturbances (cornering stiffness values, wind, . . .) affecting the vehicle. A comprehensive control scheme for an electric vehicle based on many but cheap sensors and a high degree of actuation (namely 6: 4 In Wheel Motor torques + AFS +ARS) increases performance, safety and comfort as described in [7], [12] and [13] and may also increase energy efficiency as in [8] and in [9]; it is worth to be discussed how sensor and actuator failures influence the control system performance and safety.

This contribution -as a first attempt to approach this topic- is based on the detection of failures of sensors that are essential for advanced EV lateral vehicle dynamics control. It is of outmost importance to detect sensor failures (failure detection: FD), to isolate them (failure isolation: FI) and to mitigate them

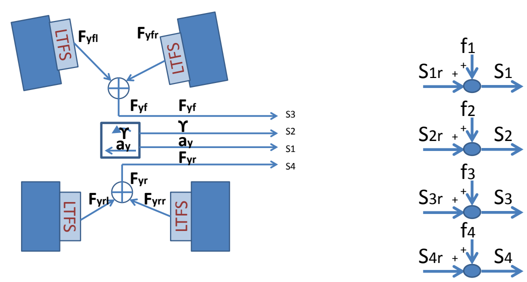

Fig. 1. Left: Sensor concept for lateral vehicle dynamics for EVs with LTFS Right: Additive sensor fault model

(failure mitigation: FM), meaning to reduce the impact of the sensor failure as much as possible. The considered electric vehicle is equipped with LTFS, lateral acceleration sensor and yaw rate sensor (optionally the roll rate sensor). The problem in the Fault Detection and Isolation in advanced lateral electric vehicle dynamics control consists in detecting accurately a sensor fault under following conditions:

- Disturbances (like unknown cross wind force)
- Uncertain parameters (mass, yaw inertia, position of center of gravity, attack point of wind force)
- Noisy sensors (especially the force sensors are affected by heavy noise)

This problem has been approached before in [1], [3], [4] and others. Quantitative aspects in FD in the parity space have been introduced (amongst others) in [2]. A good introduction in the field of model-based fault diagnosis can be found in [5] and [14]. Due to the advent of economic LTFS in the near future it seems to be reasonable to develop FDI schemes that do not rely on the knowledge of the cornering stiffness values and the vehicle velocity as opposed to the aforementioned contributions. The proposed FDI method assumes the following:

- The approach should use only basic vehicle characteriz-

978-1-4673-2420-5/12/$31.00 ©2012 IEEE

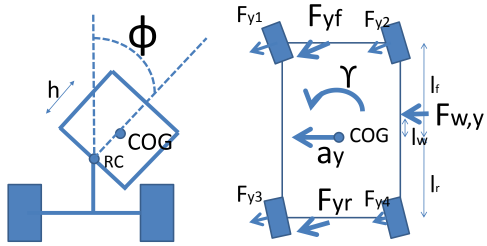

Fig. 2. Kinetic relationships for vehicle modelling, (γ: yaw rate, F_{yf}, F_{yr}: front, rear lateral force, a_y: lateral acceleration, $F_{w,y}$: crosswind force, ϕ: roll angle)

ing parameters and not parameters that are determined by estimation using sensor measurements and/or are highly time variant.

- It is assumed that only one sensor fails at a certain time. If there are no common mode causes this assumption seems to be reasonable since the probability of two sensors failing at the same time is very small or could be kept small by design.
- Cross wind affecting the vehicle should not lead to a false alarm.

In Fig. 1 the sensor concept is shown. The two front and the two rear LTF sensors are summed up to a total front and total rear lateral tire force sensor signal. This is reasonable since the important control variable for the controller are these overall forces and a discrimination within the two pair of sensors requires detailed knowledge about the road conditions for each wheel. The contribution is structured in the following way: Section II introduces the vehicle model, the FDI scheme is based on. In this particular model the lateral tire force measurements are considered as inputs and the other sensor measurements as outputs. Section III introduces the parity space and how to extract model input and output errors. Section IV deals with numeric implementation issues with residual observers and to regularize the effect of sensor noise on the detection and isolation scheme. Simulation results and experimental validations are given in section V and section VI gives short conclusions. The appendix gives on overview of the implementational issues and the computation effort needed.

II. Vehicle Modelling for Lateral Vehicle Dynamics Sensor Fault Detection

Due to the aforementioned requirements the vehicle model should be very basic and not contain derived parameters such as cornering stiffness values. By using the lateral tire forces as inputs and the other sensor values as outputs (Fig. 4) the describing equations are derived based on the kinetic relation-

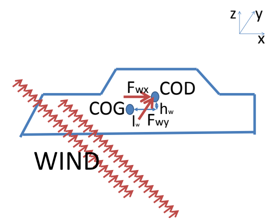

Fig. 3. Modelling of cross wind influence on the vehicle

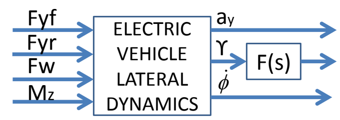

Fig. 4. Sketch of vehicle modelling for FDI purposes

ship (Fig. 2)[1]. The influence of crosswind is summarized as a lateral force $F_{w,y}$ acting at a certain distance l_w from the Center Of Gravity (COG) (Fig. 3) leading to:

$$\begin{aligned}
\dot{\mathbf{x}} &= \begin{bmatrix} \dot{\gamma} \\ \dot{\phi} \\ \ddot{\phi} \end{bmatrix} = \mathbf{A}_C\mathbf{x} + \mathbf{B}_C\mathbf{u} + \mathbf{b}_{C,0} + \mathbf{b}_{C,w}F_{w,y} \quad (1)\\
\mathbf{y} &= \begin{bmatrix} \gamma & a_y & \dot{\phi} \end{bmatrix}^T = \mathbf{C}\mathbf{x} + \mathbf{D}\mathbf{u} + \mathbf{d}_W F_{w,y}
\end{aligned}$$

with

$$\begin{aligned}
\mathbf{A}_C &= \begin{bmatrix} 0 & 0 & 0 \\ 0 & 0 & 1 \\ 0 & -\frac{K_\phi}{J_x} & -\frac{C_\phi}{J_x} \end{bmatrix}, \mathbf{B}_C \begin{bmatrix} \frac{l_f}{J_z} & \frac{-l_r}{J_z} \\ 0 & 0 \\ \frac{m_s h_s}{mJ_x} & \frac{m_s h_s}{mJ_x} \end{bmatrix},\\
\mathbf{b}_{C,o} &= \begin{bmatrix} \frac{M_z}{J_z} \\ 0 \\ \frac{M_x}{J_x} \end{bmatrix}, \mathbf{b}_{C,w} = \begin{bmatrix} \frac{l_w}{J_z} \\ 0 \\ \frac{m_s h_s}{mJ_x} \end{bmatrix}, \mathbf{u} = \begin{bmatrix} F_{yf} \\ F_{yr} \end{bmatrix},\\
\mathbf{C} &= \begin{bmatrix} 1 & 0 & 0 \\ 0 & 0 & 0 \\ 0 & 0 & 1 \end{bmatrix}, \mathbf{D} = \begin{bmatrix} 0 & 0 \\ \frac{l}{m} & \frac{l}{m} \\ 0 & 0 \end{bmatrix}, \mathbf{d}_w = \begin{bmatrix} 0 \\ \frac{1}{m} \\ 0 \end{bmatrix},
\end{aligned}$$

where m, m_S is the vehicle and vehicle sprung mass, h_s the height of the roll center, J_z, J_x the yaw and roll inertia, K_{phi}, C_{phi} the roll stiffness and roll damping and M_z, M_x [2] is the yaw and roll moment due to IWMs.

In the case of the yaw rate this simple model would lead to an open loop integration. Therefore it is advisable to use the filtered signal γ^* which can be derived from the real yaw rate γ:

$$\gamma^* = F(s)\ \gamma = \frac{s}{s+w_0}\gamma \quad (2)$$

[1]The front and rear steering angles are assumed to be small, otherwise the lateral tire force could be corrected by use of the steering angle signals.

[2]Since the driving force of IWM driven EVs can be estimated quite accurately by use of driving force observers, these quantities can be determined also.

Fault	r_1	r_2	r_3	r_4	r_5
$1: \Delta a_y$	0	1	1	1	1
$2: \Delta\gamma^*$	1	0	1	1	1
$3: \Delta F_{y,f}$	1	1	0	1	1
$4: \Delta F_{y,r}$	1	1	1	0	1
$5: F_w$	1	1	1	1	0

TABLE I
FAULT CODING SET (0:NOT INFLUENCED, 1: INFLUENCED)

with an appropriately chosen w_0.

If one does not use the roll rate sensor as additional information, the model is reduced to:

$$\begin{aligned}
\dot{\mathbf{x}} &= \left[\ \dot{\gamma}^*\ \right] = A_C x + \mathbf{B}_C \mathbf{u} + \mathbf{b}_{C,0} + \mathbf{b}_{C,w} F_{w,y} \\
\mathbf{y} &= \begin{bmatrix} \gamma^* \\ a_y \end{bmatrix} = \mathbf{C}x + \mathbf{D}\mathbf{u} + \mathbf{d}_W F_{w,y} \qquad (3)
\end{aligned}$$

with

$$\begin{aligned}
A_C &= \left[\ -w_0\ \right], \mathbf{B}_C = \begin{bmatrix} \frac{l_f}{J_z} & \frac{-l_r}{J_z} \\ 0 & 0 \end{bmatrix}, \\
\mathbf{b}_{C,o} &= \begin{bmatrix} \frac{M_z}{J_z} \\ 0 \end{bmatrix}, \mathbf{b}_{C,w} = \begin{bmatrix} \frac{l_w}{J_z} \\ 0 \end{bmatrix}, \\
\mathbf{C} &= \begin{bmatrix} 1 \\ 0 \end{bmatrix}, \mathbf{D} = \begin{bmatrix} 0 & 0 \\ \frac{l}{m} & \frac{l}{m} \end{bmatrix}, \mathbf{d}_w = \begin{bmatrix} 0 \\ \frac{1}{m} \end{bmatrix}.
\end{aligned}$$

This means a model with four inputs $r = 4$ (lateral tire forces, unknown wind force and additional yaw moment), one state $n = 1$ and two outputs $m = 2$ is obtained. In order to use the parity space model this model is approximated in discrete time[3] and the following description of the system obtained:

$$\begin{aligned}
\mathbf{x}_{k+1} &= \mathbf{A}\mathbf{x}_k + \mathbf{B}\mathbf{u}_k + \mathbf{b}_0 + \mathbf{b}_w F_{wy,k} \\
\mathbf{y}_k &= \mathbf{C}\mathbf{x}_k + \mathbf{D}\mathbf{u}_k + \mathbf{d}_w F_{wy,k} + \mathbf{f}_{Sk} + \mathbf{n}_k, \qquad (4)
\end{aligned}$$

where $\mathbf{f}_{Sk}$ contains the sensor errors of the γ^* and a_y sensor and $\mathbf{n}_k$ additional sensor noise at time instant k.

III. INTRODUCING PARITY SPACE APPROACH

The definition of the residuals in the parity space is used here for fault detection and isolation. If one collects $s + 1$ samples (s is the dimension of the parity space[4]) into the vectors $\mathbf{U}, \mathbf{Y}_m, \mathbf{U}_w$,

$$\begin{aligned}
\mathbf{U} &= \begin{bmatrix} \mathbf{u}_{k-s} \\ \vdots \\ \mathbf{u}_k \end{bmatrix}, \mathbf{Y}_m = \begin{bmatrix} \mathbf{y}_{k-s} \\ \vdots \\ \mathbf{y}_k \end{bmatrix}, \mathbf{X}_m = \dots, \\
\mathbf{U}_w &= \begin{bmatrix} F_{w,k-s} \\ \vdots \\ F_{w,k} \end{bmatrix}, \mathbf{F}_s = \begin{bmatrix} \mathbf{f}_{s,k-s} \\ \vdots \\ \mathbf{f}_{s,k} \end{bmatrix}, \mathbf{N}_s = \dots \qquad (5)
\end{aligned}$$

the measured sensor signals can be described as following:

$$\mathbf{Y}_m = \mathbf{R}\mathbf{X} + \mathbf{Q}\mathbf{U} + \mathbf{Q}_w \mathbf{U}_w + \mathbf{F}_s + \mathbf{N}_s \qquad (6)$$

[3]for example by using the Tustin discretization method.

[4]$s \geq 2$ for the use of the model with the roll rate sensor and $s \geq 1$ for the model without roll rate sensor.

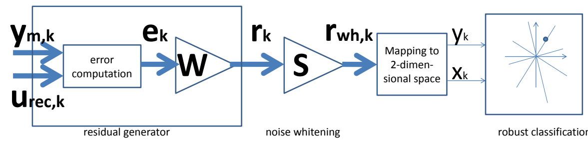

Fig. 5. Fault detection and isolation scheme (residual generator realized with residual observers)

with

$$\mathbf{R} = [\ \mathbf{C}^T \quad (\mathbf{CA})^T \quad (\mathbf{CA^2})^T \quad \dots \quad (\mathbf{CA}^s)^T\ ]^T \qquad (7)$$

and

$$\begin{aligned}
\mathbf{Q} &= \left[\ \mathbf{q_1} \quad \mathbf{q_2} \quad \mathbf{q_3} \quad \dots \quad \mathbf{q_{s+1}}\ \right] = \\
&= \begin{bmatrix} \mathbf{D} & \mathbf{0} & \mathbf{0} & \mathbf{0} & \mathbf{0} \\ \mathbf{CB} & \mathbf{D} & \mathbf{0} & \mathbf{0} & \mathbf{0} \\ \mathbf{CAB} & \mathbf{CB} & \mathbf{D} & \ddots & \mathbf{0} \\ \vdots & \vdots & \vdots & \ddots & \mathbf{0} \\ \mathbf{CA}^{s-1}\mathbf{B} & \mathbf{CA}^{s-2}\mathbf{B} & \dots & \mathbf{CB} & \mathbf{D} \end{bmatrix},
\end{aligned}$$

$$\mathbf{Q}_w = \begin{bmatrix} \mathbf{d_w} & \mathbf{0} & \mathbf{0} & \mathbf{0} & \mathbf{0} \\ \mathbf{Cb_w} & \mathbf{d}_w & \mathbf{0} & \mathbf{0} & \mathbf{0} \\ \mathbf{CAb_w} & \mathbf{Cb_w} & \mathbf{d}_w & \ddots & \mathbf{0} \\ \vdots & \vdots & \vdots & \ddots & \mathbf{0} \\ \mathbf{CA}^{s-1}\mathbf{b}_w & \mathbf{CA}^{s-2}\mathbf{b}_w & \dots & \mathbf{Cb_w} & \mathbf{d}_w \end{bmatrix}. \qquad (8)$$

Since the tire force sensor signals (that according to Fig. 4 are inputs to this system) may be faulty and noisy the following sample vector

$$\mathbf{U}_{rec} = \mathbf{U} + \mathbf{\Delta U} + \mathbf{N}_u, \qquad (9)$$

where $\mathbf{\Delta U}$ collects the LTFS faults and $\mathbf{N}_u$ the LTFS noise according to (5), can be determind and used to compute the following error vector:

$$\begin{aligned}
\mathbf{e} &= \mathbf{Y}_m - \mathbf{Q}\mathbf{U}_{rec} \\
&= \mathbf{R}\mathbf{X} + \mathbf{Q}\mathbf{U} + \mathbf{Q}_w\mathbf{U}_w + \mathbf{F}_s - \mathbf{Q}(\mathbf{U} + \mathbf{\Delta U} + \mathbf{N_u}) \\
&= \mathbf{R}\mathbf{X} + \mathbf{Q}_w\mathbf{U}_w + \mathbf{F}_s + \mathbf{N}_s - \mathbf{Q}\mathbf{\Delta U} - \mathbf{Q}\mathbf{N}_U, \qquad (10)
\end{aligned}$$

which can be multiplied with a weighting vector $\mathbf{w}_i$ in order to form the corresponding residual r_i:

$$\begin{aligned}
r_i = \mathbf{w^T}_i\mathbf{e} &= \mathbf{w^T}_i(\mathbf{R}\mathbf{X} + \mathbf{Q}_w\mathbf{U}_w + \mathbf{F}_s \\
&- \mathbf{Q}\mathbf{\Delta U}) + \mathbf{w_i^T}(\mathbf{N}_s - \mathbf{Q}\mathbf{N_u}). \qquad (11)
\end{aligned}$$

The residuals r_i are now chosen in a way to make them independent from the system states $\mathbf{X}$ and additionally from one of the sensor or actuator faults. This leads to following geometric conditions for the weighting vectors $\mathbf{w}_i$ [6]:

$$\begin{aligned}
&\mathbf{w^*}_1 \in Null\left\{\ \mathbf{R}^T\mathbf{F}_1\ \right\}; \mathbf{w^*}_2 \in Null\left\{\ \mathbf{R}^T\mathbf{F}_2\ \right\} \\
&\mathbf{w}_3 \in Null\left\{\begin{bmatrix} \mathbf{R}^T \\ \mathbf{Q}_1{}^T \end{bmatrix}\right\}; \mathbf{w}_4 \in Null\left\{\begin{bmatrix} \mathbf{R}^T \\ \mathbf{Q}_2{}^T \end{bmatrix}\right\} \\
&\mathbf{w}_5 \in Null\left\{\begin{bmatrix} \mathbf{R}^T \\ \mathbf{Q}_w{}^T \end{bmatrix}\right\}
\end{aligned}$$

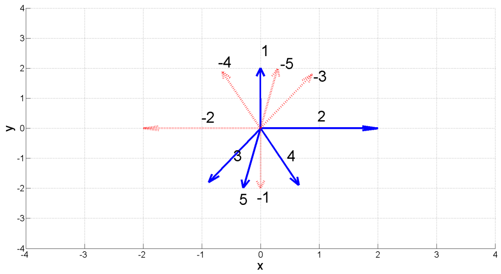

Fig. 6. Fault directions in the feature space (x, y) (1: $f_{s1} = \Delta a_y$, 2: $f_{s2} = \Delta\gamma^*$, 3: $\Delta u_1 = \Delta F_{yf}$, 4: $\Delta u_2 = \Delta F_{yr}$, 5: F_w)

with

$$\begin{aligned}
\mathbf{F}_{1\ [(s+1)m \times \frac{(s+1)m}{2}]} &= (f_{ij}),\ f_{ij} = \begin{cases} 1 & \text{if } i = 2j-1 \\ 0 & \text{elsewhere,} \end{cases} \\
\mathbf{F}_{2\ [(s+1)m \times \frac{(s+1)m}{2}]} &= (f_{ij}),\ f_{ij} = \begin{cases} 1 & \text{if } i = 2j \\ 0 & \text{elsewhere,} \end{cases}
\end{aligned}$$

$$\begin{aligned}
\mathbf{w}_1 &= \left[\begin{array}{cccccc} w_{11}^* & 0 & w_{12}^* & 0 & \dots & 0 \end{array}\right], \\
\mathbf{w}_2 &= \left[\begin{array}{cccccc} 0 & w_{21}^* & 0 & w_{22}^* & \dots & 0 \end{array}\right], \\
\mathbf{Q}_1 &= \left[\begin{array}{ccccc} \mathbf{q}_1 & \mathbf{0} & \mathbf{q}_3 & \mathbf{0} & \dots \end{array}\right], \\
\mathbf{Q}_2 &= \left[\begin{array}{ccccc} \mathbf{0} & \mathbf{q}_2 & \mathbf{0} & \mathbf{q}_4 & \dots \end{array}\right].
\end{aligned} \tag{12}$$

The so called fault coding set can be seen in Tab. I (1 means that the corresponding residual is influenced by the fault, 0 no influence). Each residual is independent of one of the sensor errors or the influence of the wind disturbance. More independence is not possible due to the dimensions of the state space n, inputs r and outputs m [5].

IV. Quantitative Parity Space Approach

As can be seen in Tab. 1 from the residual binary fault signature a single failure of a sensor can be determined. However, in real life operation it does not suffice to determine which residual is activated ($\neq 0$) or not (0) and to use this information to isolate the single fault due to sensor noise and some allowed small bias of the sensor; a more robust method is to examine the quantitative influence of a static single fault on the residuals:

$$\mathbf{S}_0 = \begin{bmatrix} \frac{\partial r_1}{\partial f_{s,1}} & \frac{\partial r_1}{\partial f_{s,2}} & \frac{\partial r_1}{\partial \Delta u_1} & \frac{\partial r_1}{\partial \Delta u_2} & \frac{\partial r_1}{\partial F_w} \\ \vdots & \vdots & \vdots & \vdots & \vdots \\ \frac{\partial r_5}{\partial f_{s,1}} & \frac{\partial r_5}{\partial f_{s,2}} & \frac{\partial r_5}{\partial \Delta u_1} & \frac{\partial r_5}{\partial \Delta u_2} & \frac{\partial r_5}{\partial F_w} \end{bmatrix} \tag{13}$$

This linear mapping from the fault to the residuals cannot be directly used to recover the single faults since it has not full rank. Actually in the case (3) approach it has only rank 2, this means that the 5 dimensional space of residuals can be mapped into a 2 dimensional space without loss of information and the fault detection and isolation be done within a two dimensional space by appropriate partitioning of this space and use of the single failure assumption.

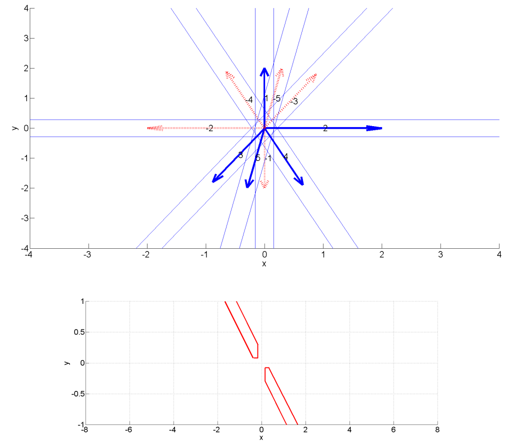

Fig. 7. Top: Regions where an unambiguous single fault detection is possible (within two blue lines, where there is no intersection with other "stripes") Bottom: Exemplary the region in the feature space for unambiguous rear lateral tire force sensor fault detection is shown.

If one considers sensors affected by noise then the covariance matrix of the noise affecting the residual vector can be described in dependence of the covariance matrix of the sensors and the matrices $\mathbf{Q}, \mathbf{W}$ according to (11):

$$\mathbf{R}_n = \mathbf{W}^T(\mathbf{R}_S + \mathbf{Q}\mathbf{R}_U\mathbf{Q}^T)\mathbf{W}$$

with

$$\mathbf{W} = [\mathbf{w}_1\ \mathbf{w}_2\ \mathbf{w}_3\ \mathbf{w}_4\ \mathbf{w}_5], \tag{14}$$

where $\mathbf{R}_S$ is the covariance matrix of the sensors (the yaw rate and lateral acceleration sensor) and $\mathbf{R}_U$ is the covariance matrix of the actuators (the lateral tire force sensors) in the parity space (compare (5)). In order to whitening the noise [11] the following decomposition of the effective noise covariance is suggested

$$\mathbf{R}_n = \mathbf{P}\mathbf{P}^T \tag{15}$$

and the following transformation of the residual vector $\mathbf{r}$

$$\mathbf{r}_{wh} = \mathbf{P}^{-1}\mathbf{r} = \mathbf{S}\mathbf{r}. \tag{16}$$

For the steady state (constant fault vector $\mathbf{f}^T = [f_{s1}, f_{s2}, \Delta u_1, \Delta u_2, F_w]$) the following relationship between the fault vector and the signal $\mathbf{r}_{wh}$ holds:

$$\mathbf{r}_{wh} = \mathbf{G}\mathbf{f} = \mathbf{S}\mathbf{r} = \mathbf{S}\mathbf{S}_0\mathbf{f}. \tag{17}$$

Since the matrix $\mathbf{G}$ has rank 2, the action of the matrix can be represented with coordinates (x, y) in a two dimensional space (which is called feature space here) by taking for example the two first column as coordinate axis and therefore leading to new coordinates:

$$\left[\begin{array}{cc} x & y \end{array}\right]^T = \{\mathbf{r}_{wh}\}_2 = (\mathbf{W_f}\mathbf{G}^\dagger\mathbf{G}(:, \mathbf{1}:\mathbf{2}))^\mathbf{T}\mathbf{f}, \tag{18}$$

where $\mathbf{W}_f$ is a matrix that weights the single faults. In Fig. 6 the single fault directions with vehicle parameters as given in section VI are indicated. It can be seen that under the noise assumptions and slight sensor deviations the ability of the

Fault	max value	det. time simulation	det. time eperiment	assumed σ_n	allowed bias
Δa_y	$0.6\frac{m}{s^2}$	$0.12s$	$0.16s$	$0.283\frac{m}{s^2}$	$0.07\frac{m}{s^2}$
$\Delta\gamma$	$0.22\frac{rad}{s}$	$0.03s$	$0.04s$	$0.01\frac{rad}{s}$	$0.03\frac{rad}{s}$
$\Delta F_{y,f}$	$300N$	$0.13s$	$0.12s$	$100N$	$10N$
$\Delta F_{y,r}$	$300N$	$0.13s$	$0.14s$	$100N$	$10N$
ΔF_w	$300N$	-	-	–	$80N$

TABLE II
SINGLE SENSOR FAULTS (MAXIMAL VALUES)

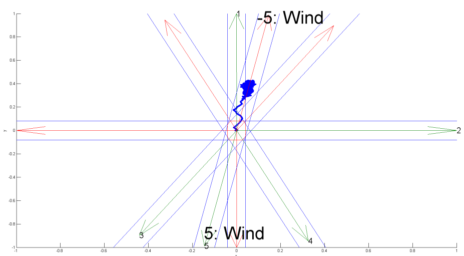

Fig. 10. Effect of a lateral wind force (simulation with noise) of $300N$ in the feature space. It is not detected as a failure in the lateral acceleration sensor.

scheme to detect the failure is reduced. In the next section the regions in this detection scheme where a sensor failure can be detected in an unambiguous way are determined.

V. Lean residual dead beat observer implementation and numerical issues

The implementation of the fault detection and isolation scheme requires a high amount of computation. However as [1] has shown a lean dead beat observer implementation is possible. By using the weight vectors $\mathbf{w}_i$ from (12) it can be directly translated to a dead beat observer by using the following observer equations [1]:

$$\mathbf{z}_{k+1} = \mathbf{G}\mathbf{z}_k + \mathbf{H}u_{,k} + \mathbf{L}\mathbf{y}_k$$
$$r_k = -\mathbf{o}\mathbf{z}_k + \mathbf{v}\mathbf{y}_k + \mathbf{q}\mathbf{u}_k$$

with

$$\begin{aligned}
\mathbf{T} &= \begin{bmatrix} \mathbf{w}_{i,1}^T & \mathbf{w}_{i,2}^T & \dots & \mathbf{w}_{i,s-1}^T & \mathbf{w}_{i,s}^T \\ \mathbf{w}_{i,2}^T & \dots & \dots & \mathbf{w}_{i,s}^T & 0 \\ \vdots & \dots & \dots & \iddots & \vdots \\ \mathbf{w}_{i,s}^T & 0 & \dots & \dots & 0 \end{bmatrix} \begin{bmatrix} \mathbf{C} \\ \mathbf{CA} \\ \vdots \\ \mathbf{CA}^{s-1} \end{bmatrix} \\
\mathbf{L}_0 &= -\begin{bmatrix} \mathbf{w}_{i,1}^T \\ \vdots \\ \mathbf{w}_{i,s-1}^T \end{bmatrix}, \mathbf{G}_0 = \begin{bmatrix} 0 & 0 & \dots & 0 \\ 1 & 0 & \dots & 0 \\ \vdots & \dots & \ddots & \vdots \\ 0 & \dots & 0 & 1 \end{bmatrix} \\
\mathbf{G} &= [\mathbf{G}_0\ \mathbf{g}], \mathbf{L} = \mathbf{L}_0 - \mathbf{w}_{i,s}^T\mathbf{g}, \mathbf{g} = 0, \\
\mathbf{o} &= [0\ \dots\ 0\ 1], \mathbf{v} = \mathbf{w}_{i,s}^T
\end{aligned} \tag{19}$$

and together with the relations $\mathbf{H} = \mathbf{TB} - \mathbf{LD}$ and $\mathbf{q} = -\mathbf{v}\mathbf{D}$ the observer is defined completely where $\mathbf{w}_i^T = [\mathbf{w}_{i,0}^T, \dots, \mathbf{w}_{s,0}^T]$ is the weight vector for each residual as defined in (12).

Fig. 11. Test vehicle FPEV2 Kanon at Hori Fujimoto Laboratory

Fig. 12. Lateral tire force sensor (NSK Ltd.)

Together with the computational efficient computation of the residuals, there must be regions in the feature space defined where a single fault can be isolated, even if there is noise affecting the sensors and other sensors are slightly biased or affected by some negligible error. Since the noise effect is whitened it can be represented as a circle in the feature space. By defining what error on the sensors is tolerable, regions in the feature space can be determined -by simply varying a single fault and define the area due to the allowed inaccuracy of the other sensors and the noise of all sensors-, where unambiguously a single sensor failure can be detected. If the residual vector in the feature space falls in the part of a single fault region, which is not an intersection with another single fault region (Fig. 7), the failure can be isolated.

VI. Simulation and experiment results

The method has been applied to a test vehicle in a simulation and an experimental setup as shown in Fig. 11. The lateral tire force sensor as shown in Fig. 12 has been used on all 4 wheels. The vehicle describing parameters were $m = 880kg, J_z = 560\frac{kgm}{s^2}$, $l_f = 0.999m$, $l_r = 0.701m$ and $l_w = -0.3m$. The vehicle has been considered during a cornering manoeuvre with radius $r = 20m$ beginning from speed $0\ km/h$ to roughly $36\ km/h$ and the different signal sensor faults artificially added to the measurement signals (compare Fig. 1). It has been assumed that the single faults occurred at a certain time $t = 15s$ and grows from 0 to its maximal value linearly

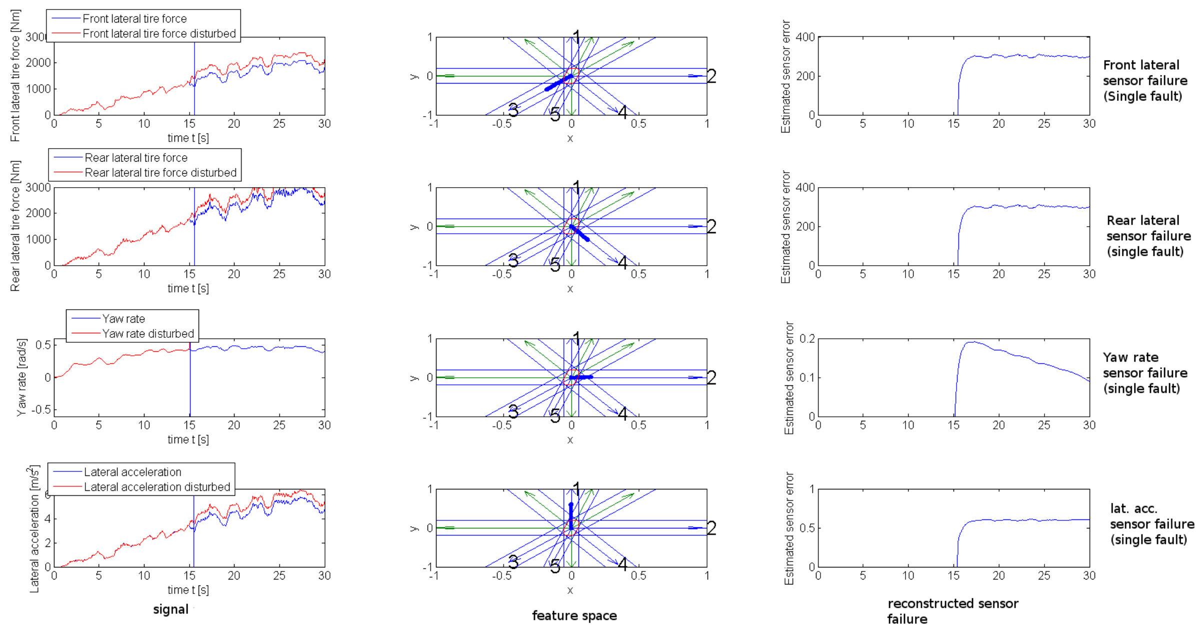

Fig. 8. Left: Simulation results (without noise) with artificially added single sensor failures (drift), their representation (middle) in the feature space and the estimated sensor fault (Faults occuring at $t = 15s$). The left diagrams show the disturbed signals (red) together with the correct signals (blue). The yaw rate sensor failure reconstruction is not possible for a constant failure as it is applied in this case (only at the beginning).

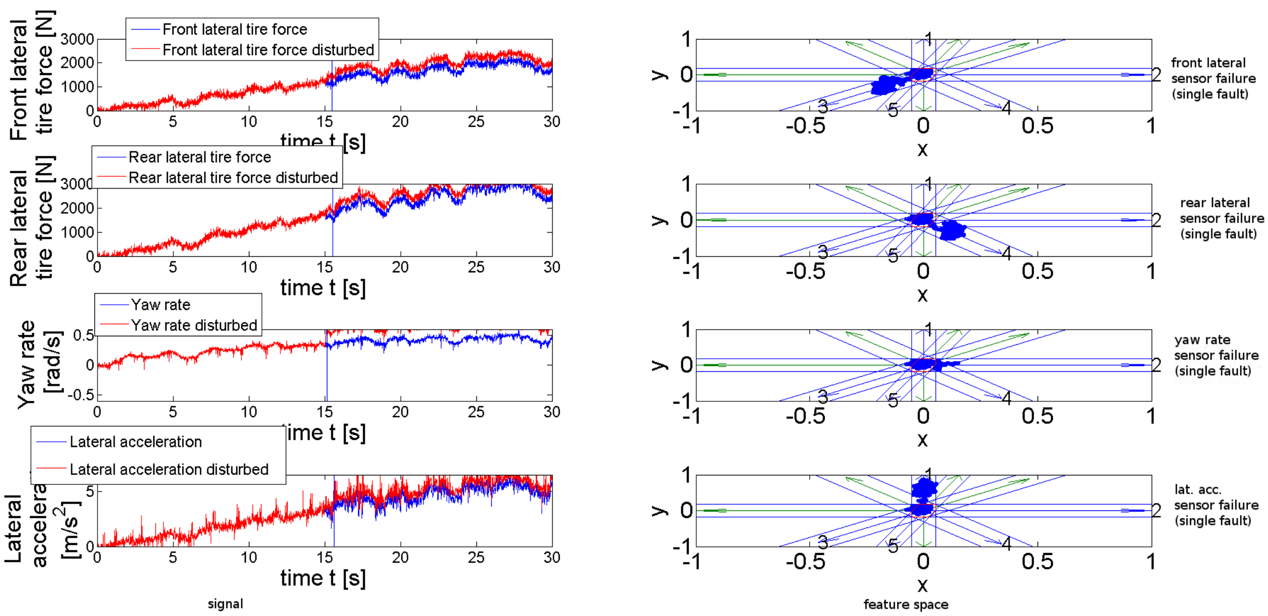

Fig. 9. Experimental results with artificially added single sensor failures (drift), their representation (right) in the feature space (Faults occuring at $t = 15s$, blue vertical line shows time instant, when error is detected). The left diagrams show the disturbed signals (red) together with the correct signals (blue).

within $125ms$, remains fixed at the maximal value and acts as a bias to the measurement signal. The fault detection and isolation scheme has been implemented with residual observers (sampling time has been set to $10ms$) and then the filtered residuals (with cut-off frequency of $10Hz^5$) mapped to the feature space according to (16), (17) and (18), where

[5]This cut off frequency is a compromise between reducing noise power and not increase detection time too much.

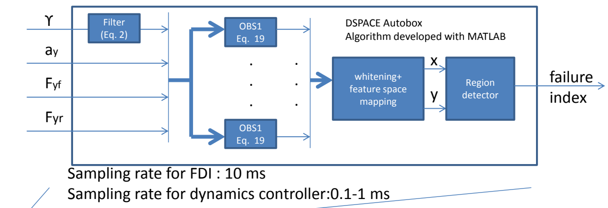

Observer implementation	Additional filters	Feature space mapper	Region detection
45 mult. (5*9) 15 add. (5*3) 5 mem. (5*1)	6 mem. (6*1) 6 mult. (6*1) 6 add. (6*1)	10 mult. (2*5) 8 add. (2*4)	40 mult. (5*4*2) 20 add. (5*4*1) 20 comp. (5*4*1)

Fig. 13. Overview of the RT implementation of the obs. based FDI scheme

a detector determined, if there is a single fault by making out in which region the residual in the feature space lies. The whole scheme (observers and detector) is implemented very efficently and runs in real time. w_0 according to (2) has been set to $3\frac{rad}{s}$. In Tab. II the maximum values of the sensor faults are given together with the achieved detection time in the simulation and experimental setup. Additionally the assumed standard deviation of the noise of each sensor are given together with the allowed where no alarm should be given. Allowed bias and noise properties determine the region in the feature spaces where an unambiguous failure detection and isolation is possible.

In Fig. 8 and Fig. 9 the results are shown (single faulty signals, feature space and reconstructed sensor error). The chosen parameters allow for a detection and isolation of the single sensor faults at a time, where (the vertical line in the diagrams on the left side) the influence of the faulty signal is still small enough to take countermeasures by the controller (reconfiguration). Strong wind can be detected and in this case no false alarm is given (Fig. 10). However the dimensionality of the model does not allow to determine unambiguously a single sensor fault in the case of crosswind.

VII. Conclusion

A scheme has been designed for lateral vehicle dynamics of electric vehicle with lateral tire force sensors for fault detection and isolation which uses ideas from classical parity space approach by taking into account sensor noise and an allowed bias or inaccuracy of the sensor. The scheme uses only general vehicle describing parameters and not estimated or very uncertain parameters like cornering stiffness values. It can be embedded in a comprehensive FDI framework for an EV. An additional sensor like a roll rate sensor would allow for another degree of freedom that would mean that the feature space would have dimensionality 3 instead of 2 allowing for creating residuals that are independent of two sensor faults or 1 sensor fault and the influence of wind (if the wind model reflects appropriately the reality). It should now be enhanced to cover not only sensor errors for the vehicle lateral dynamics, but also include additionally sensors for longitudinal dynamics (together with actuator failures). It is strongly anticipated that approaches like this together with conventional sensor plausibility checks can contribute to determine faults fast, isolate them and this knowledge be used to prevent the EVs to become unsafe in case of a sensor or actuator failure.

Acknowledgment

This research has been made possible partly by a JSPS (Japan Society for the Promotion of Science) fellowship and a kakenhi grant with number 23-00760. It was supported by the Industrial Technology Research Grant Program from the New Energy and Industrial Technology Development Organization (NEDO) of Japan (number 05A48701d), and by the Ministry of Education, Culture, Sports, Science and Technology grant (number 22246057).

The authors acknowledge the helpful comments from the anonymous reviewers.

References

[1] S. Schneider, N. Weinhold, S.X. Ding and A. Rehm, *Parity Space based FDI-Scheme for Vehicle Lateral Dynamics*, Proceedings IEEE Conference on Control Applications, Toronto, Canada, pp. 1409-1414, 2005.

[2] S. de Lira, V. Puig and Q. Quevedo, Robust LPV Model-Based Sensor Fault Diagnosis Using Relative Fault Sensitivity Signature and Residual Fault Directions Approaches in a PEM Fuel Cell, Proceedings IEEE Vehicle Power and Propulsion Conference (VPPC), 2010.

[3] A. Abdo, J. Saijai, W. Damlakhi and S. X. Ding, *An Observer-based Fault Detection Approach for Vehicle Lateral Dynamics Control System*, IFAC, Toronto, Canada, pp. 1409-1414, 2009.

[4] S. X. Ding, S. Schneider, E. L. Ding and A. Rehm, *Advanced Model-based Diagnosis of Sensor Faults in Vehicle Dynamics Control Systems*, IFAC, World Congress, Czech Republic, Vol. 16, part 1, 2005.

[5] E. Friks, *Model-based fault diagnosis applied to an SI-Engine*, PhD Thesis, University of Linkoeping, 1996.

[6] G. Strang, *Linear Algebra and its applications*, MIT Press, 1998.

[7] N. Ando and H. Fujimoto, *Yaw-rate control for electric vehicle with active front/rear steering and driving/braking force distribution of rear wheels*, Advanced Motion Control, 11th IEEE International Workshop on, pp. 726-731, 2010.

[8] Y. Chen and J. Wang, *Energy-Efficient Control Allocation with Applications on Planar Motion Control of Electric Ground Vehicles*, American Control Conference (ACC),pp. 2719 - 2724, 2011.

[9] H. Fujimoto, H. Sumiya, *Range extension control system of electric vehicle based on optimal torque distribution and cornering resistance minimization*, IECON 2011 - 37th Annual Conference on IEEE Industrial Electronics Society , pp. 3858 - 3863, 2011.

[10] E. Katsuyama, *Decoupled 3D Moment Control by In-Wheel Motor*, In Proceedings 2011 JSAE Annual Congress (Spring),(Japanese), 1-6, 2011.

[11] Madisetti, V. K. and Williams, D. B, *The Digital Signal Processing Handbook*, IEEE Press, 1997.

[12] D. Bianchi, A. Borri, G. Burgio, M.D. Di Benedetto, S. Di Gennaro,*Adaptive integrated vehicle control using active front steering and rear torque vectoring*, CDC/CCC, pp. 3557 - 3562, 2009.

[13] A. Viehweider, Y. Hori, *Vehicle Lateral Dynamics Control based on Instantaneous Cornering Stiffness Estimation and an Efficient Allocation Scheme*, MATHMOD Vienna Conference on Mathematical Modelling, 2012.

[14] R. Isermann (Editor),*Fahrdynamik-Regelung, Modellbildung, Fahrerassistenzsysteme, Mechatronik*, Vieweg publisher, 2006.

Appendix

In Fig. 13 the implementation of the scheme is shown. The algorithms are designed with MATLAB block diagrams, out of this a real time version compiled and transferred to the Autobox (DSPACE) RT system. The computational load for the RT system is very low, the scheme has a sampling time of $10ms$.